This is the accepted manuscript made available via CHORUS. The article has been published as:

Coherent x-ray scattering experiments of Pt(001) surface dynamics near a roughening transition

M. S. Pierce, A. Barbour, V. Komanicky, D. Hennessy, and H. You

Phys. Rev. B **86**, 184108 — Published 21 November 2012

DOI: 10.1103/PhysRevB.86.184108

Coherent X-ray Scattering Experiments of Pt (001) Surface Dynamics near Roughening Transition

M. S. Pierce[a,b], A. Barbour[a], V. Komanicky,[c] D. Hennessy[a], and H. You[a]

[a] Materials Science Division, Argonne National Laboratory, Argonne IL 60439

[b] School of Physics and Astronomy, Rochester Institute of Technology, Rochester NY 14623

[c] Faculty of Science, Safarik University, Košice, 04001, Slovakia

We present the results of a series of coherent x-ray scattering temperature dependent experiments from Pt (001) in high vacuum. The resulting speckled diffraction patterns are analyzed with x-ray photon correlation spectroscopy. We find that the hexagonally reconstructed Pt (001) surface exhibits orientational dynamics below 1640 K and a critical behavior as T increases to T_R = 1834 K, near the roughening transition as proposed by Abernathy, et al. [Phys. Rev. Lett. **69**, 941 (1992)]. The inverse autocorrelation time constant τ^{-1} of the surface diverges as T approaches T_R. The average integrated intensity remains constant below T_R but drops suddenly over a narrow temperature range, indicating abrupt lifting of the hexagonal reconstruction with the roughening transition. This behavior is compared to that of Au (001), for which τ^{-1} approaches a finite value as the reconstruction lifts gradually over a wide temperature range.

The physical and chemical properties of Pt and Au surfaces have been a subject of numerous important scientific studies over the years since the clean surfaces were first studied in vacuum.[1] In particular, the phenomenon of surface reconstruction has received a great deal of attention because it is one of the most fundamental mechanisms governing metal surfaces. As Pt and Au share many similar properties, understanding the differences that arise in experimental studies can often provide particularly useful information. Both are face centered cubic (FCC) metals with similar lattice constants, and their (100) surfaces undergo a quasi-hexagonal surface reconstruction.[2,3] Furthermore, in spite of a considerable difference in melting temperatures, the reconstruction lifts at approximately the same point when the temperatures are measured as a percent of their respective melting points.

However, there are substantial differences between the two surfaces. Perhaps the most recognized difference is the reactivity of Pt compared to the nobility of Au for large samples.[4] There are also significant differences in correlation lengths, the behavior of the terraces with respect to temperature, and how the reconstruction rotates and lifts.[2] In our recent studies, we also found a difference in their dynamic behaviors. The hex reconstruction of Au (001) surface lifts gradually over a considerable temperature range to a disordered (1×1) surface.[5] The hex reconstruction has a considerable amount of defects over a wide temperature range. However, that of the Pt (001) surface lifts quite abruptly with a sudden increase of step motion as temperature reaches to a critical temperature.[6] The Pt (001) surface remains highly ordered, free from surface defects right to the point of lifting.

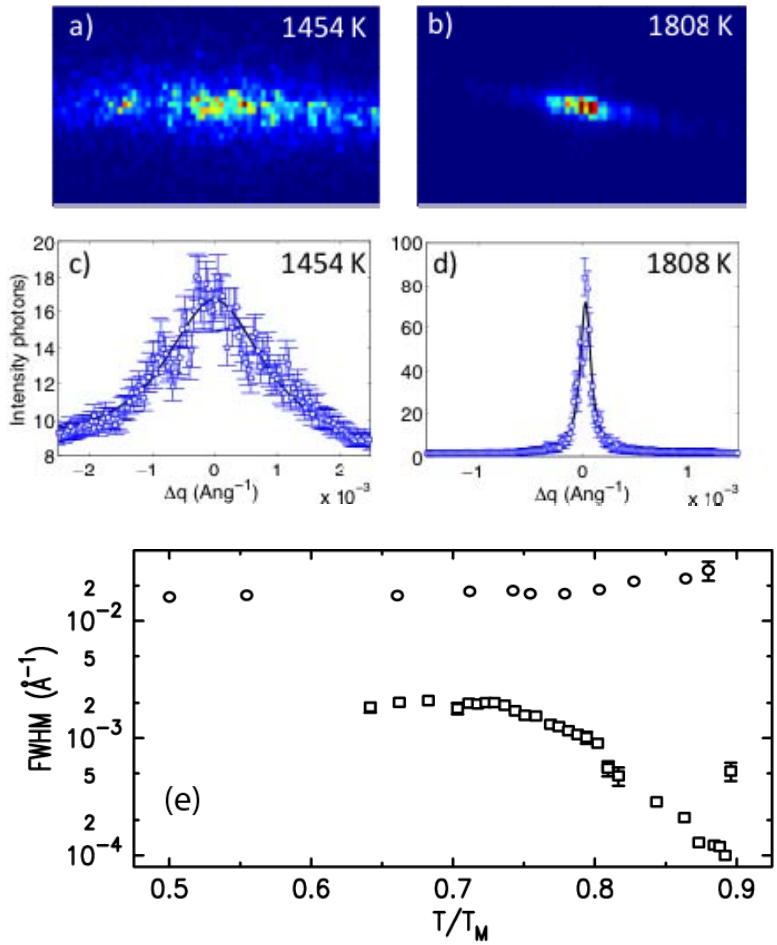

Figure 1. Observed scattering patterns for Pt (001) at two different temperatures. The low-temperature pattern (a) is considerably more diffuse than the high-temperature pattern (b). While the width and peak intensity both change, the total scattering is approximately the same for both temperatures. Panels c) and d) show an average along the horizontal directions shown with simple Lorentzian fits. (e) FWHM vs. T/T_M for Pt (squares) and Au (circles).

We have performed a series of coherent x-ray scattering (CXS) experiments and x-ray photon correlation spectroscopy (XPCS) analysis from Pt (001) and compared with our earlier studies of Au (001). We find that the autocorrelation time of Pt (001) surface exhibits a clear dependence upon temperature, qualitatively similar to Au (001). However, unlike Au, we find the Pt surface exhibits a critical behavior as *T* increases to the temperature of lifting the hex reconstruction. In order to facilitate comparison

between Pt and Au, we may refer to temperatures by reduced temperatures, T/T_M, where T_M is the melting temperature.

Our experiments were performed at 8ID of the Advanced Photon Source (APS), using a small vacuum chamber mounted directly to the diffractometer. A single bounce monochromator was used to select photons with energy of 7.36 keV. Precision slits, nominally 10×10 μm^2, were used to select a desirable level of coherence. Incident coherent flux on the sample would typically be ~ 10^9 photons /sec with a few thousand arriving in the detector each second. A low noise x-ray charge coupled device (CCD) with a pixel size of 20×20 microns was positioned at 2.1 m from the sample for data collection. A radio frequency (RF) induction heater was used to control the sample temperature in a chamber with pressure at ~10^{-6} Torr or less. A residual gas analyzer (RGA) was also used to monitor the elemental and molecular components of the vacuum.

Bulk annealing of the platinum crystals was performed by an *ex-situ* induction heater for 10 hr at 1900 K in argon/hydrogen flow (3% hydrogen, high purity) at ambient pressure. This procedure produces well oriented surfaces free of surface contamination.[7] The samples would then be stored in Millipore ultrapure deionized water (18 M□cm, Total Organic Carbon <5 ppb) for transfer into the chamber. During transfer, the vacuum chamber would be over pressured using high purity nitrogen, the sample mounted and secured on the pedestal, and the chamber sealed. Each sample would then be annealed at high temperature (~1200 K) for several hours prior to data collection to further clean the

surface. The samples have a nominal miscut of 0.1° or less. The bulk lattice parameter was used to determine the temperature of the sample.[8]

Typical scattering patterns from Pt, collected at the surface-sensitive (001) anti-Bragg condition at two different temperatures, are shown in Fig. 1 (a) and (b). While the total integrated intensity is similar, the width of the scattering signal below 1620 K (c) is much larger than above 1620 K (d), which shows a significantly narrower, higher peak with fewer speckles visible. The temperature dependence of the full-width at half-max (FWHM), determined by fitting a Lorentzian profile to the scattering peak, for both Pt (001) and Au (001) are shown in Fig. 1(e). The Pt surface exhibits much higher ordering than the Au surface. In fact, even the most disordered Pt patterns collected showed a narrower distribution than all but the absolute highest ordered Au surfaces we studied previously. This concentration of the scattering intensity allows for roughly a decade of improvement in temporal sensitivity for Pt compared to Au. For Au, the FWHM gradually increases, indicating that the surface becomes more disordered as the phase transition from hex to 1×1 is approached. In contrast, for Pt, the FWHM narrows considerably and systematically as the temperature is increased until the reconstruction lifts at $T/T_M = 0.89$. The Pt surface reconstruction lifts entirely within one step of our temperature resolution, showing no evidence of coexistence between a hex phase and a disordered 1×1 phase.

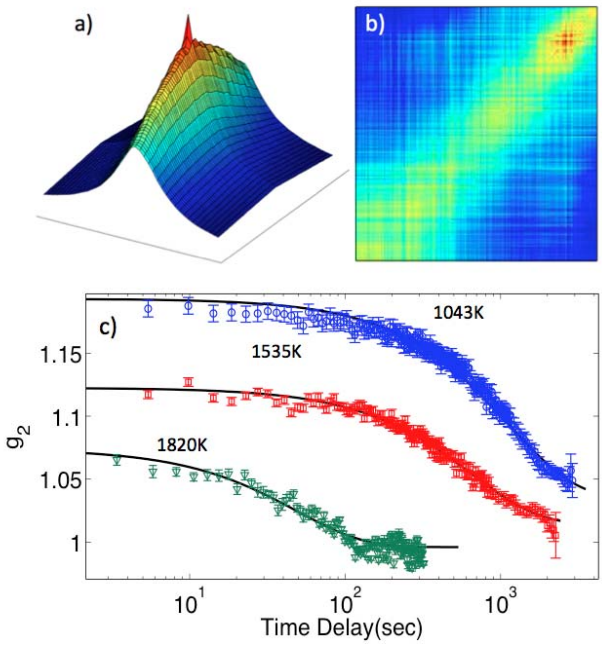

Figure 2. Top, pre-analysis of the speckle patterns. (a) shows the autocorrelation of a single image. The sharp feature is the signal of interest. Its ratio to the background represents the speckle contrast, and the width of the peak is inversely related to the speckle size. (b) shows an example of a two-point correlation calculation. (c) Example auto-correlation measurements for Pt are shown for 3 different temperatures. The data at 1535 K and 1043 K are offset by +0.02 and +0.04, respectively, for clarity.

To investigate the dynamics of the surface, we performed a time-time auto-correlation analysis of the speckle patterns. The first step in such an analysis is to restrict the data set to a continuous portion that can be used for equilibrium dynamics measurements for a given temperature. A constant average intensity and position of the (001) reflection were both necessary conditions for thermal equilibrium. For a subset of data matching those conditions, we performed a series of single image auto-correlations and two-point correlation analysis to provide further confidence in establishing equilibrium data sets. Examples of such analyses are given in Fig. 2 (a) and (b), respectively. Single image autocorrelation (a) provides for a measure of the contrast in the image, as well as capturing the convolution of the incoherent background with itself. Two-point

correlation analyses[9] (b) were performed to detect any experimental non-equilibrium behavior and exclude such frames. The two-point correlation analysis also quickly identified regions of the oscillatory data due to step flow motion at very high temperatures.[6] From the remaining data, which show relatively continuous equilibrium dynamics, a traditional time-time autocorrelation was performed.

The normalized auto-correlation was calculated on a pixel by pixel basis from

$$g_2(\Delta t) = \frac{\langle I(t+\Delta t) I(t) \rangle}{\langle I(\Delta t) \rangle \langle I(t) \rangle}. \qquad (1)$$

using a symmetric normalization scheme.[10,9] Auto-correlations from single pixels were then averaged together over several neighboring pixels to optimize counting statistics without affecting the time resolution. Typically the calculation involved calculating a smoothed average that was subtracted prior to the auto-correlation in order to produce a meaningful measure of contrast. Only pixels with at least 3 photons on average were used in the autocorrelation.

Examples of the auto-correlation data for Pt are shown in Fig. 2(c). Three different temperatures are shown with a general trend of increasing decorrelation rates, hence faster changes, with increasing temperature. We can fit a simple exponential decay for the autocorrelation as $g_2(\Delta t) = 1 + \beta e^{-\Delta t/\tau}$. Here τ is the temperature-dependent decorrelation time constant and β is the contrast in the speckle patterns. The contrasts are often small even after properly averaged because of partially coherence and imperfect detectors in the experiments. Also, Debye-Waller factor decreases the contrast at higher temperatures. However, the time constants are generally robust and sensitive to the

surface dynamics as presented in a logarithmic time scale (c). Due to the relatively narrow profile of the Pt scattering peak and the strong intensity per pixel, the Pt auto-correlation data tend to be of higher quality than those from Au (001)[5]. This not only resulted in better statistics, but also allows for up to a factor of 10 improvement in time resolution.

We report only the results obtained above 900 K. While this is not a true ultra-high vacuum (UHV) experiment, we are confident that our results are not affected by the high vacuum nature of the experimental setup. At high temperature, all the elemental and molecular species monitored by the residual gas analyzer in the chamber should have desorbed.[11,12] Also, the surface is continuously refreshed by evaporation on time scales of seconds or minutes.[6] Therefore, we expect that the surface should remain clean free from contamination. In addition, our results reproduce the results of earlier UHV x-ray scattering experiments.[13,14,15,16]

Temperature dependent behavior of τ is shown in Fig. 3. There are two temperature regions of interest, shown in the data separated at 1620 K. Two regions are evident in the semi-log plot covering three decades and two regions are shown separately in (b) and (c) for clarity. Below this temperature, the hex domains are slightly misoriented from the (110) directions and above this they are aligned.[13] The two regions are also evident in FWHM shown in Fig. 1(e). Above 1620 K, we observed significant narrowing in the width of the Pt (001) scattering reflection. That is, once aligned, the lateral long-range order of the hex reconstruction increases with increasing temperature. The subsequent

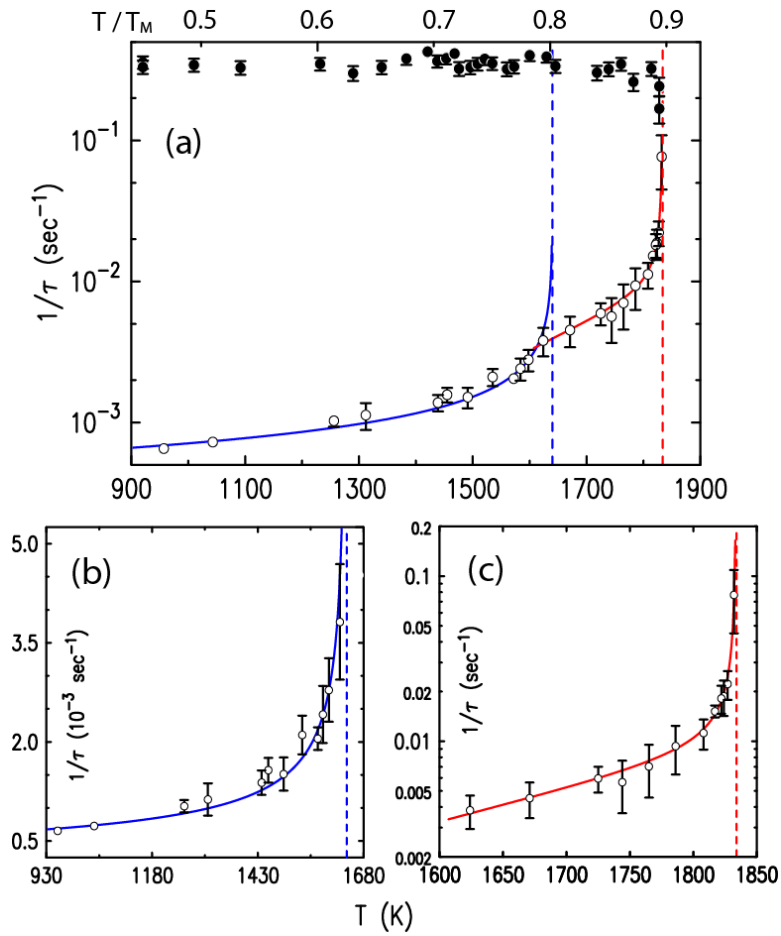

Figure 3. a) $1/\tau$ (open circles) and integrated intensity (solid circles) vs. T. The blue and red curves are the fits to the orientational and roughening transitions, respectively. The transition temperatures (1640 K and 1834 K) are shown by dashed vertical lines. (b) in a linear scale and (c) in a semi-log scale show each fits separately for clarity.

increase of the lateral ordering indicates also that the bulk-to-hex interaction becomes gradually less important than lateral interactions within the hex layer as the temperature increases.

The low temperature part of τ shown in Fig. 3 is consistent with orientational fluctuations. At low temperature, the hex domains are rotated by ~1° away from (110) directions. As T approaches 1600 K, the rotation angle decreases rapidly and becomes zero at 1680 K.[13] For this reason, we assume that the dynamics of the surface below

1620 K seen in our data is dominated by orientational fluctuation of the domains. Since the rotation angle behaves like $\theta \approx |1 - T/T_O|^{1/2}$ in temperature, we believe that the orientational thermal fluctuation should behave like $\frac{\partial\theta}{\partial T} \approx |1 - T/T_O|^{-1/2}$. Therefore, the inverse decorrelation time was heuristically fit with the same power-law behavior $\tau^{-1} \approx |1 - T/T_O|^{-1/2}$ with the fit value for the orientational transition temperature (T_O) being 1640(5) K. The fit works well, albeit qualitatively.

The temperature behavior above 1620 K is particularly interesting. τ^{--1} diverges as T approaches another transition temperature. At first, it appears similar to the hex-to-(1×1) transition temperature observed for Au (001) with increasing τ^{--1} with increasing temperature.[5] However, as the temperature approaches the transition the behavior is substantially different; $\tau^{—1}$ for Au (001) approach a constant value while $\tau^{—1}$ for Pt (001) diverges. We believe this behavior of Pt (001) is probably due to the roughening transition, as previously suggested for Pt (001) surface[14] and for its vicinal surfaces.[15] In both cases, the hex reconstruction remains until the transition takes place. This is different from the behavior of the Au (001) surface[16] for which lifting of the hex reconstruction takes place without any evidence of a roughening transition.

In a standard theory of roughening transition,[17,18] the free energy of steps near the roughening transition approaches zero with $f^s = f^0 \exp\left[-\sqrt{A/(T_R - T)}\right]$, and the step creations and fluctuations become increasingly easier as $T \rightarrow T_R$. As we have done for the

case of Au (001) surface,5 we describe the temperature dependence with an Arrhenius form as $\tau^{-1} \sim \exp\left(-f^{s}/k_{\mathrm{B}}T\right)$ using the predicted free energy. Then,

$$\tau^{-1} \sim \exp\left[-f^{0}\exp\left(-\sqrt{A/(T_R - T)}\right)/T\right]. \qquad (2)$$

Since we do not expect this is valid for low temperature, we fit only the data above 1620 K. The best fit of the data above 1600 K to Eq. (1) is shown by the red solid line in Fig. 3 (a) and (c). The fit value for f^{0} is 11(2) 10^{3} K. This indicates that the step energy f^{s} is close to 1 eV when the temperature is sufficiently below the fit value of T_R= 1833.8(4) K. This value is close to the average theoretical value of 1.35 eV.[19] The value for the non-universal constant A is 0.6(2) K. This indicates that the free energy is 90 % of f^{0} for the temperatures tens of degrees below T_{R}, (most temperature range) and appreciably different from it only when the temperature is as close to T_{R} as ~20 K.

It is also important to note that the total intensity, shown in Fig. 3(a), is roughly constant below T_R. Based on this and the FWHM shown in Fig. 1(e), we see that the average terrace width does not change much until the temperature reaches very close to the transition. The total intensity does not change much even when step edges fluctuate and increase in length, as long as the average terrace width does not change much. Therefore, we can conclude that the roughening transition proceeds mainly via step meandering and fluctuation until the temperature approaches T_{R}. Close to the transition, however, it is expected that the steps proliferate and the intensity decreases. This can be seen in the data point closest to T_{R} for the total intensity in Fig. 3(a). The proliferation of steps is probably responsible for the significant deviation of the measured step velocity above

1800 K.[6] Note also that the last data point of τ^{-1} jumps, and the fit line captures the point. We found no other functional form that behaves like Eq. (1) capable of including the last data point. For temperatures above T_R, we were unable to obtain data of sufficient quality for XPCS. The drop of the intensity and the fast time-scales for surface evolution result in insufficient signal within the image exposure times needed.

It is interesting to compare our study with the study by Abernathy et al.[14] In their study, the strong experimental evidence for a roughening transition was rather cautiously presented because of an apparent discrepancy in the fluctuation length scale above T_R to computer simulations. Although our study focuses below T_R and does not provide more information on the length scale issues, we believe our study provides an additional support for the roughening transition based on the temperature-dependent dynamics. In addition, let us consider other related phenomena besides the roughening transition, such as pre-roughening,[20] surface melting,[21] and surface-melting mediated pre-roughening.[22] Our measurements will not differentiate pre-roughening from roughening. The intensity at the anti-Bragg condition is insufficiently sensitive to distinguish multi step heights from a single step height. For surface melting, the situation can also be very similar. Our experiment is mainly sensitive to the step edge fluctuations, whether they occur because the system approaches melting or roughening. The main conclusion we can make here is that the fit using the step free energy predicted by the roughening transition works well for the decorrelation time constants.

In conclusion we have measured the decorrelation rate of the surface of Pt (001) over a temperature range from 800K to 1835K. The observed decorrelation rates are faster than those measured for Au (001) at the same T/T_M. At sufficiently high temperatures, we observe critical behavior of the decorrelation time even though the average intensity does not show any significant changes. We were able to fit the decorrelation rates using the prediction of step free energy for the well-known roughening transition. We find T_R to be 1833.8(4) K, which is also in agreement with the previous study.[14]

This work and use of the Advanced Photon Source were supported by the U.S. Department of Energy, Office of Basic Energy Sciences, under Contract No. DE-AC02-06CH11357. The work at Safarik University was supported by Slovak grant VEGA 1/0782/12. The authors wish to thank T. Einstein for discussion and references, and A. Sandy for his assistance with the experiments at 8ID of the APS.

REFERENCES

[1] S. Hagstrom, H.B. Lyon, and G.A. Somorjai, Phys. Rev. Lett. **15**, 491 (1965).

[2] D. Gibbs, B.M. Ocko, D.M. Zehner, and S.G.J. Mochrie, Phys. Rev. B **42**, 7330 (1990); *ibid*,. B **38**, 7303 (1988); D. L. Abernathy, S.G.J. Mochrie, D.M. Zener, G. Grübel, D. Gibbs, Phys. Rev. Lett. **69**, 941(1992); Phys. Rev. **B 45**, 9272 (1992).

[3] N. Takeuchi, C.T. Chan and K.M. Ho, Phys. Rev. Lett. **63**, 1273 (1989).

[4] G. Ertl, *Reactions at Solid Surfaces*, Wiley, 2009.

[5] M.S. Pierce, K.C. Chang, D. Hennessy, V. Komanicky, M. Sprung, A. Sandy, and H. You, Phys. Rev. Lett. **103**, 165501 (2009).

[6] M.S. Pierce, D.C. Hennessy, K.C. Chang, V. Komanicky, J. Strzalka, A. Sandy, A. Barbour, and H. You, App. Phys. Lett. **99**, 121910 (2011).

[7] V. Komanicky, K. C. Chang, A. Menzel, N. M. Markovic, H. You, X. Wang, D. Myers, Journal of The Electrochemical Society, **153** B446-B451 (2006).

[8] F.C. Nix and D. MacNair, Phys. Rev. **60**, 597 (1941). F.C. Nix and D. MacNair, Phys. Rev. **61**, 74 (1942).

[9] G. Brown, P.A. Rikvold, M. Sutton, M. Grant, Phys. Rev. E 56, 6601 (1997).

[10] D. Lumma, L. B. Lurio, and S. G. J. Mochrie, and M. Sutton, Rev. Sci. Instrument 71, 3274 (2000).

[11] J.F. Weaver, H.H. Kan, and R.B. Shumbera, J. Phys. Condens. Matter 20, 184015 (2008).

[12] R.J. Behm, P.A. Thiel, P.R. Norton, and G. Ertl, J. Chem. Phys. **78**, 7437 (1983); P.A. Thiel, R.J. Behm, P.R. Norton, and G. Ertl, *ibid*, 7448 (1983).

[13] D.L. Abernathy, S.G.J. Mochrie, D.M. Zehner, G. Grübel, D. Gibbs, Phys. Rev. B **45** 9272 (1992).

[14] D.L. Abernathy, S.G.J. Mochrie, D.M. Zehner, G. Grübel, D. Gibbs, Phys. Rev. Lett. **69**, 941 (1992).

[15] G.M. Watson, D. Gibbs, D.M. Zehner, M. Yoon, S.G.J. Mochrie, Phys. Rev. Lett. **71**, 3166 (1993).

[16] G.M. Watson, D. Gibbs, D.M. Zehner, M. Yoon, S.G.J. Mochrie, Surf. Sci. **407**, 59 (1998).

[17] J. Villain, D.R. Grempel, J. Laujoulade, J. Phys. F **15**, 809 (1985).

[18] H. van Beijeren, I. Nolden, *Structure and Dynamics of Surfaces II*, p259, ed. W. Schommers, P. von Blankckenhagen, Springer-Verlag, Berlin, 1989.

[19] A. Tchernatinsky and J.W. Halley, Phys. Rev. B 83, 205431 (2011).

[20] Koos Rommelse and Marcel den Nijs, Phys.Rev.Lett. **59**, 2578 (1987).

[21] L. Pietronero, E. Tosatti, Sol. Stat. Comm. **32**, 255 (1979).

[22] E.A. Jagla, S. Prestipino, and E. Tosatti, Phys. Rev. Lett. **83**, 2753 (1999).